Time-dependent Fourier grid Hamiltonian method for modelling real-time quantum dynamics: Theoretical models and applications

SATRAJIT ADHIKARI and S P BHATTACHARYYA*

Department of Physical Chemistry, Indian Association for the Cultivation of Science, Jadavpur, Calcutta 700 032, India

Abstract. A local grid method for modelling real-time quantum dynamical events is formulated. The formulation is straightforward for 1-D systems. For more than one dimension, appeal has to be made to mean-field approximation of the appropriate kind. The simplest mean-field model results in time-dependent Hartree–Fourier grid method. The relationship of the proposed method with some other methods available in the literature is examined. A few examples of numerical applications dealing with (i) the dynamics of dissociation and ionization processes in diatoms and atoms respectively and (ii) tunnelling dynamics in the intramolecular H-atom transfer phenomenon are presented.

1. Introduction

With the spectacular advent of experimental ultra-fast laser spectroscopy, the theoretical problem of minutely explaining and understanding the temporal evolution of states of a microsystem under precisely defined conditions has become a hotly pursued area of research in chemical physics (Noid *et al* 1981; Ratner and Gerber 1986; Bandrauk 1988; Phillips *et al* 1992; Kudla and Schatz 1993). Theoretical development which has been fast and varied may be broadly classified into the following types: (a) the classical trajectory method; (b) the method of semiclassical dynamics; (c) quantum coupled channel method; (d) time-dependent quantum mechanical methods. Let us clarify at the very outset that our purpose here will be to concentrate on a method of the type (d). Since we intend to deal frequently with very strong external or internal perturbations, we shall not be concerned with any quantum mechanical method of perturbative origin. Our interest will be confined to quantum mechanical methods that are potentially exact.

Exact time-dependent quantum mechanical methods have been rather slow to develop. Initially, the time-dependent problems used to be solved by expanding the evolving states of interest in a basis set, diagonalizing the Hamiltonian matrix, and finally using these eigenvalues and eigenvectors for propagating the state in time. A serious impediment to the success of this strategy has been the limitation imposed by the size and types of basis sets that can be used (Newberger and Noid 1983). As an alternative, basis-set-free or grid methods for solving time-dependent Schrödinger

---

*For correspondence

equation have been proposed and profitably utilized. The utility of grid methods is dependent on the ability to determine the eigenvalues and eigenvectors on the same grid on which the propagation in time is carried out (McCullough and Wyatt 1969, 1971). A new strategy that has become quite popular has recently been proposed by Kosloff (Kosloff and Tal-Ezer 1986; Kosloff 1988). Central to Kosloff's strategy is the idea that both ψ and $H\psi$ can be represented as vectors whose components measure the values of the functions on an appropriate (pre-set) grid of points in the coordinate space. The time-dependent Schrödinger equation is then solved by the application of a pseudospectral or fast Fourier transform (FFT) method for the spatial derivatives while adopting either an explicit differencing scheme or exponentiation for time propagation (Feit and Fleck 1983). Recently, a matrix representation of $\hat{H}$ in this vector space has been proposed by Marston and Balint-Kurti (1989) and Balint-Kurti *et al* (1991) leading to what has now become known as the Fourier grid Hamiltonian (FGH) method for calculating the bound-state eigenfunctions and eigenvalues with high accuracy. The FGH method is a special case of the discrete variable representation (DVR) method (Light *et al* 1985; Whitnell and Light 1989) but is much simpler to implement. A complex scaled FGH method too has been proposed and used with success (Chu 1990). Convergence with respect to the number of grid points, which is essentially arbitrary, is quite fast, thus giving it an edge over the FFT-based methods. In what follows, we explore the possibility of constructing time-dependent generalization of the FGH method in one (Adhikari and Bhattacharyya 1992; Adhikari *et al* 1992) as well as many dimensions (Adhikari *et al* 1993; Dutta *et al* 1993) and apply them to suitable model problems.

2. The time-dependent FGH methods

2.1 *TDFGH method in one dimension*

We start with the time-dependent Schrödinger equation for a system described by an $(1 + 1) - d$ Hamiltonian $\hat{H}(x, t)$ $(\hbar = 1, e = 1, m = 1)$

$$
\begin{aligned}
i \frac{\partial \psi(x, t)}{\partial t} &= H\psi(x, t) \\
&= [\hat{H}_0 + \hat{V}(x, t)]\psi(x, t) \\
&= [\hat{T} + \hat{V}_0(x) + \hat{V}(x, t)]\psi(x, t).
\end{aligned}
\tag{1}
$$

In (1) $\hat{H}$ has been partitioned into a time-independent Hamiltonian $\hat{H}_0 (= \hat{T} + \hat{V}_0(x))$ and a time-dependent potential $\hat{V}(x, t)$. It is straightforward to invoke the FGH recipe (Marston and Balint-Kurti 1989) for calculating the eigenfunctions and eigenvalues of $\hat{H}_0$

$$
H_0|\phi_i^0(x)\rangle = \varepsilon_i^0|\phi_i^0(x)\rangle, \quad i = 1, 2, \ldots, n_x,
$$

where n_x is the number of discrete grid points on the x-coordinate axis used for representing $|\phi_i^0(x)\rangle$. It is to be noted that the continuous range of coordinate values of x has been replaced in the FGH method by a uniform grid of discrete values $x_i = i\Delta x$, where Δx is the uniform spacing between the grid points. The basic bras

and kets of this discretized coordinate space give the value of the wave function at the designated grid points (Marston and Balint-Kurti 1989)

$$\langle x_i | \phi \rangle = \phi(x_i) = \omega_i \quad \text{(say)}. \tag{2}$$

The normalization condition for ϕ on this regular grid is given by

$$\sum_{i=1}^{n_x} \phi^*(x_i)\phi(x_i)\Delta x = 1, \tag{3}$$

while the identity operator $\hat{I}_x$ in this representation is given by

$$\hat{I}_x = \sum_{i=1}^{n_x} |x_i\rangle \Delta x \langle x_i|, \tag{4}$$

and the orthonormality condition on the grid reads

$$\Delta x \langle x_i | x_j \rangle = \delta_{ij}. \tag{5}$$

The ω_i's of (2) are obtained via the standard variational recipe. We note at this point that the same representation can be used for representing the time-dependent state function $\psi(x, t)$ of (1) on the same grid leading to a time-dependent Fourier grid Hamiltonian method (TDFGH). The only change to be made for this is to make the grid amplitudes (ω_i) time-dependent,

$$|\psi(x, t)\rangle = \sum_{i=1}^{n_x} |x_i\rangle \Delta x \omega_i(t), \tag{6}$$

and invoke the Dirac–Frenkel variational principle (Dirac 1930; Frenkel 1934). We then have,

$$\left\langle \delta\psi(x, t) \left| H - i\frac{\partial}{\partial t} \right| \psi(x, t) \right\rangle = 0. \tag{7}$$

Since $\omega_i(t)$s are to be treated as variational parameters, (7) immediately gives

$$\sum_i \sum_j \Delta x \, \delta\omega_i(t) \left\langle x_i \left| H - i\frac{\partial}{\partial t} \right| x_j \right\rangle \Delta x \omega_j(t) = 0. \tag{8}$$

Treating the variations $\delta\omega_i(t)$ as arbitrary and independent, we have from (8) the following stationary conditions:

$$\sum_j \Delta x \{ \langle x_i | H | x_j \rangle \omega_j(t) - i\langle x_i | x_j \rangle \Delta x \dot{\omega}_j(t)| = 0, \tag{9}$$

where $i = 1, 2, \ldots, n_x$ and $\dot{\omega}_j = \partial\omega_j/\partial t$.

Using orthonormality conditions on the grid, we have

$$\langle x_i | x_j \rangle \Delta x = \delta_{ij},$$

which simplifies (9) to

$$\sum_j \Delta x \{\langle x_i|H|x_j\rangle \omega_j(t)\} - i\dot\omega_i(t) = 0, \quad i = 1, 2, \ldots, n_x. \tag{10}$$

The evolution equation for the grid amplitudes now becomes

$$\dot\omega_i(t) = \frac{1}{i} \sum_j \Delta x \{\langle x_i|H|x_j\rangle\} \omega_j(t), \quad i = 1, 2, \ldots, n_x$$

$$= \frac{1}{i} \sum_j \Delta x \{\langle x_i|H_0|x_j\rangle + \langle x_i|V(x,t)|x_j\rangle\} \omega_j(t). \tag{11}$$

Using the FGH recipe for calculating the matrix elements on a grid of odd number of points we have

$$(H_0)_{ij} = \langle x_i|H_0|x_j\rangle$$

$$= \frac{1}{\Delta x} \left\{ \sum_{i=1}^{n_x} \frac{2\cos(2\pi l(i-j)/n_x)}{n_x} T_l + V(x_i)\delta_{ij} \right\}, \tag{12}$$

where

$$T_l = \frac{\hbar^2}{2m_0}(l\Delta k)^2, \quad \Delta k = 2\pi/m_x\Delta x, \text{ and } 2m = n_x - 1.$$

The matrix elements of the perturbation $V(x, t)$ can be similarly evaluated as soon as its form is specified. For example, if $V(x, t) = \varepsilon_0 x \cos(\omega t)$ we have $\langle x_i|V(x,t)|x_j\rangle = \varepsilon_0 v(x_i)\delta_{ij}\cos(\omega t)$. Similar expressions can be worked out for perturbing potentials of a different form. Equation (11) can be numerically integrated provided reasonable initial values $\{\omega_i(t = 0)\}$ are specified. If we assume $V(x, t) = 0$ at $t = 0$, the grid amplitudes for the FGH eigenstate of H_0 can provide the initial values of $\omega_i(t)$s. It may be noted that the same set of TDFGH equations were deduced earlier by us (Adhikari *et al* 1992) without involving the Dirac–Frenkel variational principle. The present derivation connects the TDFGH method with the philosophy of time-dependent variational principle in general and paves the way for its easy multi-dimensional generalizations.

2.2 *TDFGH method in two dimensions*

For a system with two coupled spatial degrees of freedom, one is forced to invoke some kind of mean-field approximation. For coupled oscillators, the simplest time-dependent mean-field approximation is the time-dependent Hartree approximation (Makri and Miller 1987; Alimi and Gerber 1990; Coalson 1990; Messina and Coalson 1990). In the context of FGH representation, the corresponding scheme may be called Hartree-time-dependent-Fourier grid Hamiltonian approximation. The model may be described as follows.

Let the system be described by a 2-d Hamiltonian (H) where

$$\hat H = \hat T_x + V(\hat x) + \hat T_y + V(\hat y) + \lambda V(x, y, t)$$

$$= h_x^0 + h_y^0 + \lambda V(x, y, t) = H_0 + \lambda V(x, y, t). \tag{13}$$

Let us assume that $\lambda = 0$ to start with, and the perturbation is switched on at $t = 0$. At $t = 0$, the system is therefore described by a non-interacting 2-d Hamiltonian H_0 where

$$H_0 = h_x^0 + h_y^0. \tag{14}$$

The ground state of the system at $t = 0$ can therefore be represented as a product of the ground states of h_x^0 and h_y^0 which may be supposed to be known exactly following the FGH recipe for determining bound states of 1-d Hamiltonians:

$$h_x^0 |\phi_0^0(x,t)\rangle = \varepsilon_{0x}^0 |\phi_0^0(x,t)\rangle,$$
$$h_y^0 |x_0^0(y,t)\rangle = \varepsilon_{0y}^0 |x_0^0(y,t)\rangle, \tag{15}$$

where

$$|\phi_0^0(x,t)\rangle = \sum_{i=1}^{n_x} \omega_{i0}^x(t) |x_i\rangle \Delta x,$$

$$|x_0^0(y,t)\rangle = \sum_{j=1}^{n_y} \omega_{j0}^y(t) |y_j\rangle \Delta y,$$

ω_{i0}^x's being the time-dependent amplitudes of $\phi_0^0(x,t)$ at the ith grid point on the x-axis while ω_{j0}^y's represent the corresponding quantities for $x_0^0(y,t)$ on the y-axis. Up to this point, the time dependence of $\omega_{i0}^x(t)$ or $\omega_{j0}^y(t)$ has been implicitly assumed to be as follows:

$$\omega_{i0}^x(t) = \omega_{i0}^x(0)\exp(-i\varepsilon_{0x}^0 t)$$
$$\omega_{j0}^y(t) = \omega_{j0}^y(0)\exp(-i\varepsilon_{0y}^0 t) \tag{16}$$

As the perturbation $V(x,y,t)$ is switched on ω_{i0}^x and ω_{j0}^y begin to evolve in time non-trivially, the time evolution now being entirely controlled by the nature of the perturbing potential $V(x,y,t)$. The ground state of H in the mean-field approximation can therefore be represented by

$$|\tilde{\psi}_0(x,y,t)\rangle = |\tilde{\phi}_0^0(x,t)\tilde{x}_0^0(y,t)\rangle$$
$$= \sum_{i=1}^{n_x} \sum_{j=1}^{n_y} \tilde{\omega}_{i0}^x(t)\tilde{\omega}_{j0}^y(t)|x_i y_j\rangle \Delta x \Delta y. \tag{17}$$

Now invoking once again the Dirac–Frenkel time-dependent variational principle for $|\tilde{\psi}_0(x,y,t)\rangle$, we have

$$\left\langle \delta\tilde{\psi}_0(x,y,t) \left| H - i\frac{\partial}{\partial t} \right| \tilde{\psi}_0(x,y,t) \right\rangle = 0, \tag{18}$$

or

$$\left\langle \delta\tilde{\phi}_0^0(x,t)\tilde{x}_0^0(y,t) \left| h_x^0 + h_y^0 + \lambda V(x,y,t) - i\frac{\partial}{\partial t} \right| \tilde{\phi}_0^0(x,t)\tilde{x}_0^0(y,t) \right\rangle$$
$$+ \left\langle \tilde{\phi}_0^0(x,t)\delta\tilde{x}_0^0(y,t) \left| h_x^0 + h_y^0 + \lambda V(x,y,t) - i\frac{\partial}{\partial t} \right| \tilde{\phi}_0^0(x,t)\tilde{x}_0^0(y,t) \right\rangle = 0, \tag{19}$$

where

$$\delta\tilde{\phi}_0^0(x,t) = \sum_i \delta\omega_{i0}^x(t)|x_i\rangle\Delta x \text{ and } \delta\tilde{x}_0^0(y,t) = \sum_j \delta\omega_{j0}^y(t)|y_j\rangle\Delta y,$$

in the FGH representation that we are using. Assuming the variations $\delta\tilde{\phi}_0^0(x,t)$ and $\delta\tilde{x}_0^0(x,t)$ to be independent and arbitrary, (19) leads us to two sets of equations, viz.

$$\left\langle \tilde{x}_0^0(y,t) \left| h_x^0 + h_y^0 + \lambda V(x,y,t) - i\frac{\partial}{\partial t} \right| \tilde{\phi}_0^0(x,t)\tilde{x}_0^0(y,t) \right\rangle = 0, \tag{20}$$

$$\left\langle \tilde{\phi}_0^0(x,t) \left| h_x^0 + h_y^0 + \lambda V(x,y,t) - i\frac{\partial}{\partial t} \right| \tilde{\phi}_0^0(x,t)\tilde{x}_0^0(y,t) \right\rangle = 0. \tag{21}$$

From (20) we can easily get

$$\{h_x^0 + \tilde{\varepsilon}_y^0 + \lambda\langle\tilde{x}_0^0(y,t)|V(x,y,t)|\tilde{x}_0^0(y,t)\rangle\}|\tilde{\phi}_0^0(x,t)\rangle$$

$$= i\left\langle x_0^0(y,t) \left| \frac{\partial}{\partial t} \right| \tilde{\phi}_0^0(x,t)\tilde{x}_0^0(y,t) \right\rangle, \tag{22}$$

where

$$\tilde{\varepsilon}_0^y = \langle\tilde{x}_0^0(y,t)|h_0^y|\tilde{x}_0^0(y,t)\rangle.$$

Now defining a y-averaged potential $V(x,\bar{y},t)$ in the FGH representation as

$$V(x,\bar{y},t) = \langle\tilde{x}_0^0(y,t)|V(x,y,t)|\tilde{x}_0^0(y,t)\rangle$$

$$= \sum_i \sum_j \tilde{\omega}_{i0}^{y*}\tilde{\omega}_{j0}^y V(x,y_i,t)\delta_{ij}\Delta y,$$

$$\{h_x^0 + \tilde{\varepsilon}_y^0 + \lambda V(x,\bar{y},t)\}|\tilde{\phi}_0^0(x,t)\rangle = i\{\langle\tilde{x}_0^0(y,t)|\dot{\tilde{x}}_0^0(y,t)\rangle$$

$$+ \langle\tilde{x}_0^0(y,t)|\tilde{x}_0^0(y,t)\rangle|\dot{\tilde{\phi}}_0^0(x,t)\rangle\}. \tag{23}$$

If we now assume that

$$|\langle\tilde{x}_0^0(y,t)|\tilde{x}_0^0(y,t)\rangle = 1 \text{ and } \langle\tilde{x}_0^0(y,t)|\dot{\tilde{x}}_0^0(y,t)\rangle = 0,$$

for any value of t making $\tilde{x}_0^0$ unique thereby, (23) easily leads ot an effective Schrödinger equation in 1-D:

$$H_x^{\text{eff}}|\tilde{\phi}_0^0(x,t)\rangle = i|\dot{\tilde{\phi}}_0^0(x,t)\rangle, \tag{24}$$

where

$$H_x^{\text{eff}} = h_x^0 + \tilde{\varepsilon}_y^0 + \lambda V(x,\bar{y},t). \tag{25}$$

In a similar manner, we can arrive at another effective 1-D Schrödinger equation, starting with (21):

$$H_y^{\text{eff}}|\tilde{x}_0^0(y,t)\rangle = i|\dot{\tilde{x}}_0^0(y,t)\rangle, \tag{26}$$

where

$$H_y^{\text{eff}} = h_y^0 + \tilde{\varepsilon}_x^0 + \lambda V(\bar{x},y,t), \tag{27}$$

where $V(\bar{x},y,t)$ represents x-averaged potential. Following the 1-D TDFGH recipe,

we can now easily convert (24) and (26) into equations representing evolution of the grid amplitudes. Thus, using the fact that

$$|\tilde{\phi}_0^0(x,t)\rangle = \sum_{i=1}^{n_x} \tilde{\omega}_{ix}^0(t)|x_i\rangle \Delta x$$

$$|\tilde{x}_0^0(y,t)\rangle = \sum_{j=1}^{n_y} \tilde{\omega}_{jy}^0(t)|y_j\rangle \Delta y$$

in (24) and (26), and projecting on $\langle x_k|(k=1,2,\ldots,n_x)$ and $\langle y_m|(m=1,2,\ldots,n_y)$ respectively, we have the Hartree-TDFGH equation in two-dimensions (x,y):

$$i\dot{\tilde{\omega}}_{kx}^0 = \sum_{i}^{n_x} \langle x_k|H_x^{\text{eff}}|x_i\rangle \tilde{\omega}_{ix}^0 \Delta x, \quad (k=1,2,\ldots,n_x) \tag{28}$$

$$i\dot{\tilde{\omega}}_{my}^0 = \sum_{j}^{n_y} \langle y_m|H_y^{\text{eff}}|y_j\rangle \tilde{\omega}_{jy}^0 \Delta y, \quad (m=1,2,\ldots,n_y). \tag{29}$$

Instead of projecting on the basic bra-states $\langle x_k|$ and $\langle y_m|$ on the grids, we could have made a further application of Dirac–Frenkel variational principle with H_x^{eff} and H_y^{eff} and arrived at (28) and (29) directly. However, the present method of derivation keeps the connection with our previous derivation of TDFGH equation in 1-D transparent. Equations (28) and (29) can be integrated numerically and apply equally well to potentials with or without explicit time dependence, provided Fourier series expansion of the potential is possible both in the spatial and time coordinates. Although the derivation given above explicitly refers to a 2-D Hamiltonian, it is perfectly general and can be applied with equal facility to the n-dimensional case.

Let us suppose that our system has n mutually orthogonal spatial degrees of freedom such that the kinetic energy operator is diagonal in the corresponding conjugate momentum representation. Let these spatial degrees of freedom be denoted by $q_1, q_2, \ldots, q_n$. Then the trial n-dimensional Hartree-FGH wavefunction for the ground state may be represented as

$$|\tilde{\psi}_0(q_1,\ldots,q_i,\ldots,q_n)\rangle = |\tilde{\phi}_0^1(q_1,t)\tilde{\phi}_0^2(q_2,t)\cdots\tilde{\phi}_0^n(q_n,t)\rangle, \tag{30}$$

where

$$\tilde{\phi}_0^i(q_i,t) = \sum_r \omega_{r0}^{q_i}(t)|q_{ri}\rangle \Delta q_i \text{ and } \omega_{r0}^{q_i} = \langle q_{ri}|\tilde{\phi}_0^i(q_i,t)\rangle. \tag{31}$$

Now following the same time-dependent variational strategy as adopted for the 2-D problem, we arrive at a set of n effective 1-D Schrödinger equations,

$$H_{\text{eff}}^{q_i}|\tilde{\phi}^i(q_i,t)\rangle = i\frac{\partial}{\partial t}|\tilde{\phi}^i(q_i,t)\rangle, \tag{32}$$

for $i=1,2,\ldots,n$. The corresponding TDFGH equations to be solved are

$$i\dot{\omega}_{r0}^{q_k} = \sum_s \langle q_{rk}|H_{\text{eff}}^{q_k}|q_{sk}\rangle \omega_{s0}^{q_k}(t), \tag{33}$$

for $k=1,2,\ldots,n$ and $r=1,2,\ldots,n(q_k)$, where $n(q_k)$ is the number of grid points on

the kth coordinate axis (q_k) and H^k_{eff} contains an effective potential averaged over all the spatial degrees of freedom except q_k. One can further generalize the trial function and arrive at multi-configuration TDFGH equations which are, however, more difficult to solve.

2.3   *Comparative features of TDFGH method and other methods*

The TDFGH methods proposed have some specially postive features. One important point to note is that the method proposed is free from the problems associated with basis set methods just as the fast Fourier transform method (Kosloff 1988) is, but, unlike the FFT based method, it can work with an arbitrary number of grid points and is much simpler to implement. This fact coupled with its equal applicability to both time-independent and time-dependent potentials may eventually establish TDFGH methods as superior to many other available methods for carrying out quantum dynamical calculation, for example the split operator method of Feit and Fleck (1983) in conjunction with the fast Fourier transform method. It may be noted that the use of the FGH representation in the formulation presented in the preceding sections has the advantage of preserving the diagonality of the time-dependent effective potential for the specific problem which naturally eliminates the requirement of diagonalizing the Hamiltonian matrix at each time step. This need to diagonalize the energy matrix at each time step is a serious impediment to the study of quantum dynamics in strongly coupled systems. The TDFGH formulation, on the other hand, requires only the diagonal terms of the effective Hamiltonian matrix to be advanced in time in order to effect the time evolution of the discrete coordinate representative of the wavefunction (ψ) on the specified grid under the action of H or H^{eff}. It would be appropriate to mention here that the TDFGH formulation has an edge over the standard time-dependent perturbative formulation of the problem concerned. Thus, the perturbative formulation in a basis of the eigenstates of H_0 would lead to an apparently simple formulation in the sense that only the matrix elements of the time-dependent perturbing potential are required to compute the time-dependent amplitudes. In our formulation, however, the need to perform the quadratures repeatedly for constructing the *nondiagonal* time-dependent coupling potential matrix no longer exists.

It is quite clear that the present formulation is closely connected with the fast Fourier transform split operator methods (Feit *et al* 1982; Kosloff 1988). In fact, the FGH formulation of the kinetic energy operator developed by Marston and Balint-Kurti (1989) which we have used in our time-dependent formulation provides an explicit, finite and analytic representation of the FFT procedure in which the three operations implied by the transformation $F^{-1}TF$ have been condensed into a single analytical expression of the matrix element represented as a finite sum over cosine functions and is therefore much simpler to implement. Again, the long-time propagator of Kosloff is applicable only to time-independent potentials while the short-time propagator is meant for explicit time-dependent Hamiltonians; the TDFGH formulation is global and applies with equal facility to both types of problems. But a suitable integrator is needed for numerically integrating the equations giving the grid point amplitudes as a function of time. Although the fourth-order Runge–Kutta method will generally solve the problem in many cases, the Bulirsch–Stoer integrator

(Stoer and Bulirsch 1980) is a better tool for strongly coupled systems (Adhikari *et al* 1993).

3. Applications of the TDFGH method

3.1 *Dissociation of a diatom in a high intensity IR laser field*

Since the system has a single vibrational mode, we can effectively represent it by an appropriate Morse oscillator. Specifically, we consider here a Morse oscillator representing O–H$^-$ ($D_0 = 0.1747$ a.u., $x_e = 1.8330$ a.u, $\beta = 1.1930$ a.u). The unperturbed Hamiltonian is therefore given by

$$H_0 = \frac{P^2}{2m} + D_0\{1 - \exp(-\beta(x - x_e))\}^2, \quad (m = 1632.0 \text{ a.u.}). \tag{34}$$

The laser–molecule interaction term $V(x, t)$ is represented by

$$V(x, t) = \mu e \cdot x \varepsilon_0 \cos \omega t, \quad \hbar\omega = 0.30 \text{ eV}, \tag{35}$$

where the dipole moment function μ is given by

$$\mu = \mu_0 \exp(-(x^2/\alpha x_e^2)). \tag{36}$$

The value of α is so chosen as to reproduce the dipole moment of O–H$^-$ in the ground-state vibrational level ($v = 0$), μ_0 being the average ground-state dipole moment. Equations in (11) have been integrated with fourth-order Runge–Kutta integrator on a grid of 99 points ($\Delta x = 0.1111$ a.u.).

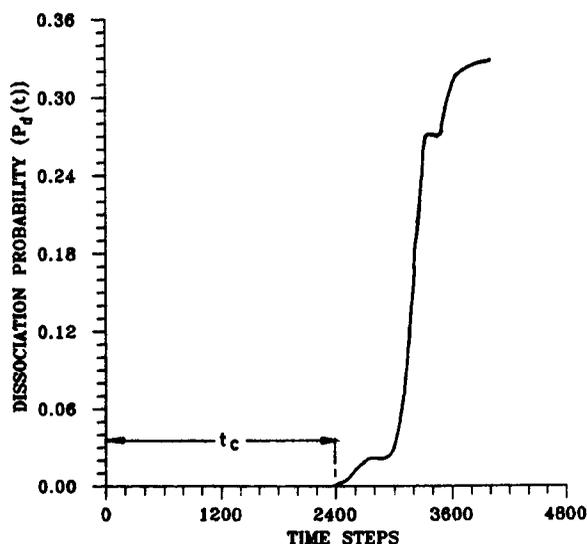Figure 1 shows the computed dissociation probability $P_d(t)$ as a function of time

Figure 1. The dissociation probability $P_d(t)$ of O–H$^-$ modelled by an appropriate Morse oscillator as a function of time, for $\varepsilon_0 = 0.17$ a.u. One time step = 0.006 fs, $\hbar\omega = 0.3$ eV.
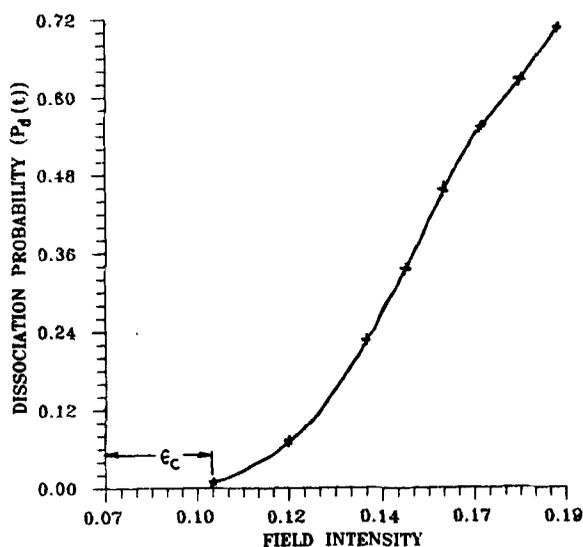
Figure 2. The dissociation probability $P_d(\tau)$ of $O-H^-$ up to a given time (τ) shown as a function of ε_0. Note the existence of a critical field strength for the onset of noticeable dissociation.

for $\varepsilon_0 = 0.17$ a.u. It is interesting to note that the dissociation probability shows a definite induction period of approximately 15 femtoseconds. From our previous experience (Adhikari and Bhattacharyya 1992) with LiH and HF, we tend to conclude that the time threshold is sensitive to the detailed features of the Morse oscillator (i.e. shallow or deep well, high or low curvature). Figure 2, on the other hand, shows the computed dissociation probability up to a given time as a function of ε_0. Here also, the dissociation probability shows the existence of a definite intensity threshold only beyond which P_d is appreciably large. The threshold value of $\varepsilon_0 (= \varepsilon_0^e)$ for $O-H^-$ turns out to be equal to 0.12 a.u. Thus, the laser-induced dissociation of a diatom is seen to be characterized by the existence of a definite bottlenecking problem which can be overcome only by increasing the intensity of the radiation to very high values. The other alternative is to use chirped pulses with lower intensity (Chelkowski and Bandrauk 1990; Chelkowski *et al* 1990). Figure 3a shows the energy absorbed by OH^- as a function of time for $\varepsilon_0 = 0.17$ a.u. while figure 3b depicts the *average number of photons* (of energy $\hbar\omega$) absorbed which shows a staircase-like structure signifying the onset of progressively higher-order processes at different stages of the time evolution.
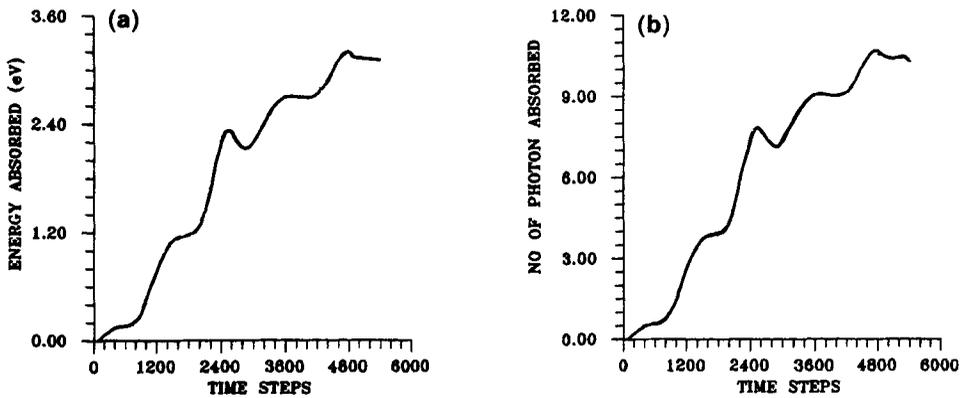
3.2 *Ionization of 1-d hydrogenic atoms in a high-intensity laser field*

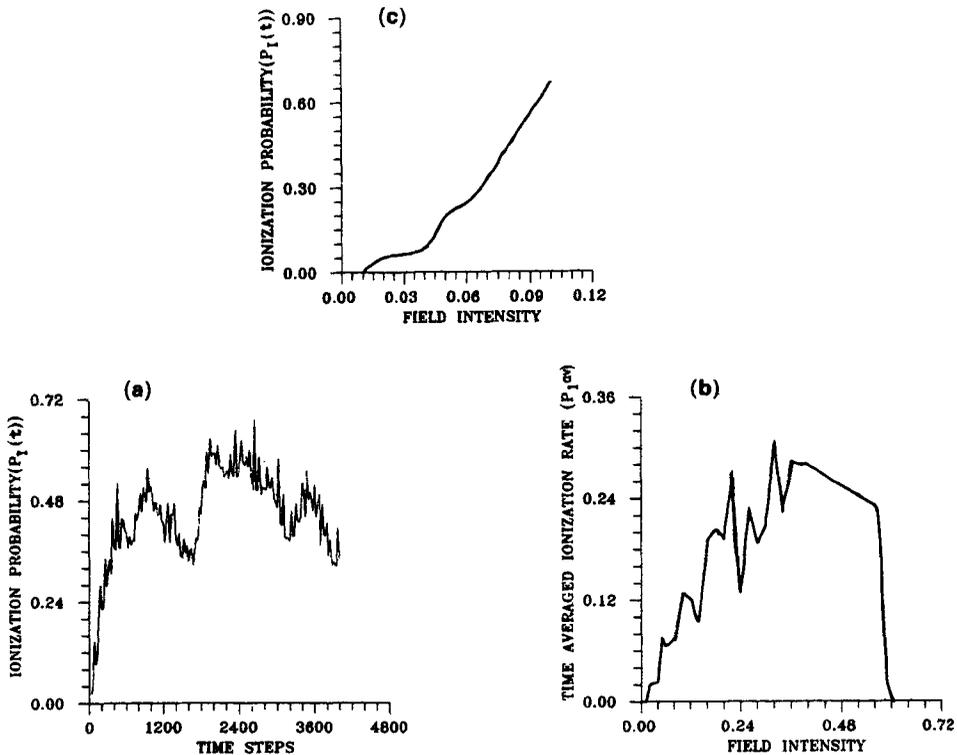The model Hamiltonian for this system is represented as

$$H = H_0 + e \cdot x \varepsilon_0 \cos \omega t, \quad \hbar\omega = 10.0 \, eV \tag{37}$$

and

$$H_0 = \frac{P^2}{2m} - \frac{\lambda}{|x|}. \tag{38}$$

Figure 3. (a) The energy absorbed by $O-H^-$ shown as a function of time for $\varepsilon_0 = 0.17$ a.u., $\hbar\omega = 0.3$ eV, $\Delta t = 0.006$ fs. (b) The number of photons absorbed under the same conditions shown as a function of time for $\varepsilon_0 = 0.17$ a.u.

Figure 4. (a) The computed ionization probability of one-dimensional H atom $P_1(t)$, displayed as a function of time for $\varepsilon_0 = 0.10$ a.u, $\hbar\omega = 10.0$ eV and $\Delta t = 0.01$ fs. (b) The dependence of the time-averaged ionization rate P_1^{av} on the strength (ε_0) of the electric field of radiation is shown. Note the suppression of the rate at high field strength. (c) The existence of an intensity threshold for the laser-induced ionization of H atom displayed by the $P_1-\varepsilon_0$ profile.

For our problem, we have taken $\lambda = 1.0$ a.u. (H atom). Figure 4a shows the computed ionization probability $P_I(t)$ as a function of time while figure 4b displays the dependence of the time-averaged ionization rate P_1^{av} on the strength (ε_0) of the electric field of the laser $\left(P_I(t) = 1 - \sum_{i=1}^{n_b} |\langle \psi(x,t)|\phi_i^0 \rangle|^2, n_b \text{ being the number of bound levels of } H_0 \right)$. The profile of $P_1^{av}(\varepsilon_0)$ shows the existence of a threshold field (ε_0^c), and more interestingly it clearly exhibits an abrupt suppression of ionization rate at high fields, a phenomenon that has been hotly pursued in recent times (Burnett *et al* 1991; Grochmalicki *et al* 1991). Figure 4c exhibits the dependence of the ionization probability $(P_I(t))$ on ε_0. The existence of a threshold intensity of ionization can be clearly seen from figure 4c.

3.3 *Chemical dynamics in two dimensions*

As a model we consider a H-atom transfer reaction, say in malonaldehyde (figure 5). It can be visualized as an effectively two-dimensional problem and then modelled by a 2-D Hamiltonian $H(Q,q)$ (Bosch *et al* 1990)

$$H(Q,q) = V_0 \left[\frac{1}{2m}\dot{Q}^2 + \frac{1}{2m}\dot{q}^2 + Q^4 - 2Q^2 - CQ^2q + \frac{1}{2}\omega^2 \left(q + \frac{C}{\omega^2} \right)^2 + 1 - \frac{C^2}{2\omega^2} \right], \quad (39)$$

where all the parameters except V_0 are dimensionless $(C = 0.86, \omega = 0.71,$ scaled time $\tau = \Omega_0 t, \Omega_0 = 1 \times 10^{15} s^{-1},$ $V_0 = 18.0 \text{kcal/mol}, m = 5367.3$ a.u., the adiabatic barrier height $V^{\#} = V_0(1 - C^2/2\omega^2) = 4.98 \text{kcal/mol},$ q and Q are mass-weighted coordinates which may be approximately identified with the O–O stretching motion (figure 5) and the motion of H with respect to the O–O centre, respectively. The potential part of $H(Q,q)$ is displayed in figure 6a. At $t = 0$, the system has been described by a wavefunction (ψ_L) localized in the left well (figure 6b). The localized wavefunction ψ_L at $E = 1.17235 \times 10^{-2}$ eV has been constructed by superposing the two lowest eigenfunctions of $H(Q,q)$ which are practically degenerate energetically. The probability of the initially localized state (ψ_i) leaking through the barrier into the right well can be given by

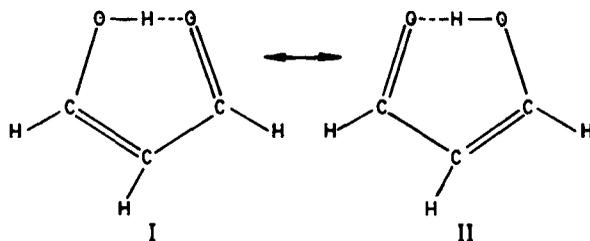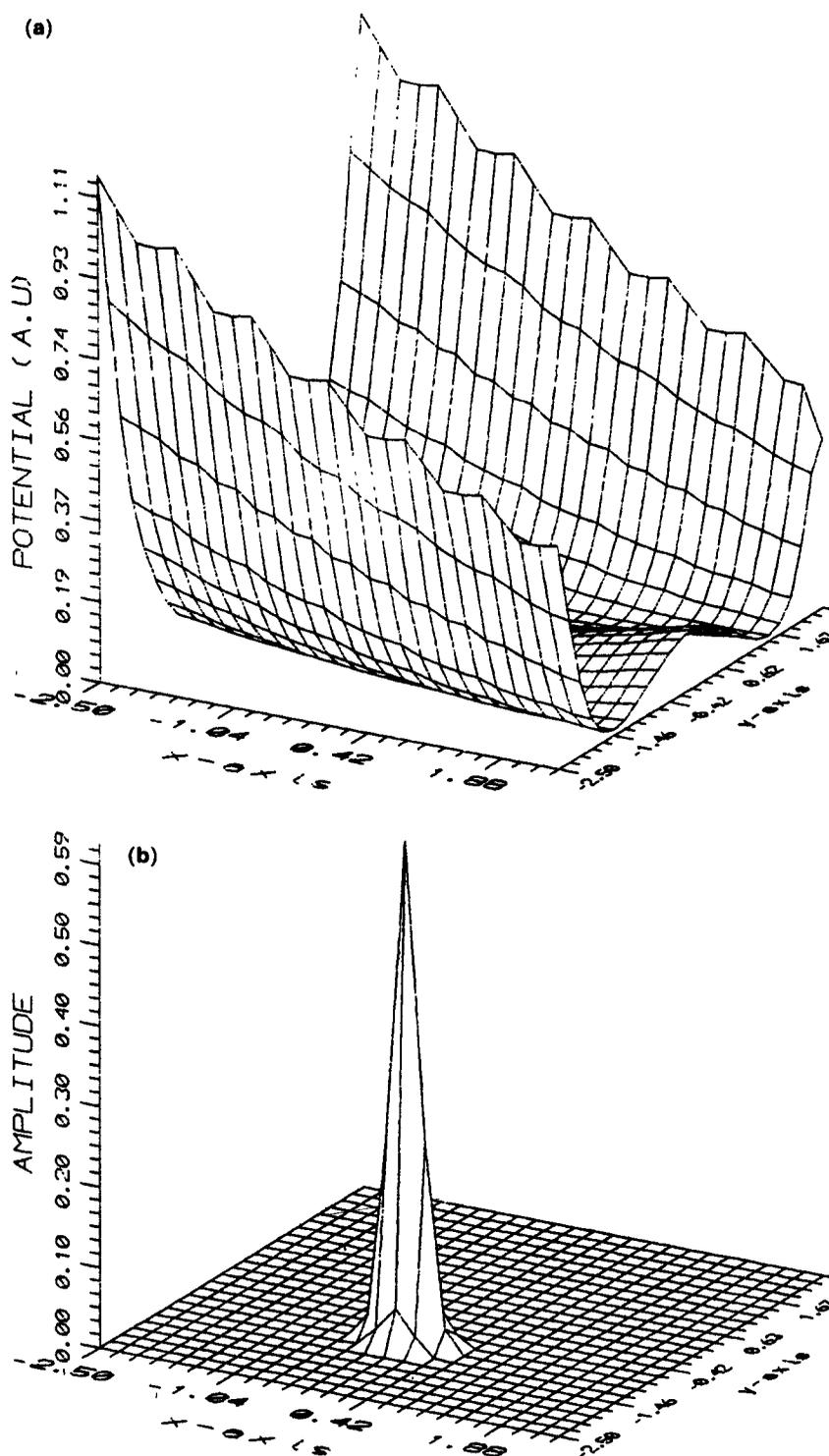$$P(t) = 1 - \int_q \int_Q |\psi_L(Q,q,t)|^2 \, dQ \, dq, \quad (40)$$

Figure 5. The two forms of malonaldehyde (MA) between which H-atom transfer takes place.

(a)

(b)

Figure 6. (a) The potential part of $H(Q,q)$, the model Hamiltonian describing the proton transfer in MA, shown graphically. (b) The localized wave function in the left well at $t = 0$.

where the integration limits are so chosen as to define the left well perimeters correctly. In the FGH representation used by us the integration is replaced by summation over discrete grid points in the q and Q dimensions:

$$P(t) = 1 - \sum_{r=m_1}^{m_2} \sum_{s=n_1}^{n_2} |\omega_{r0}^q|^2 |\omega_{s0}^Q|^2, \tag{41}$$

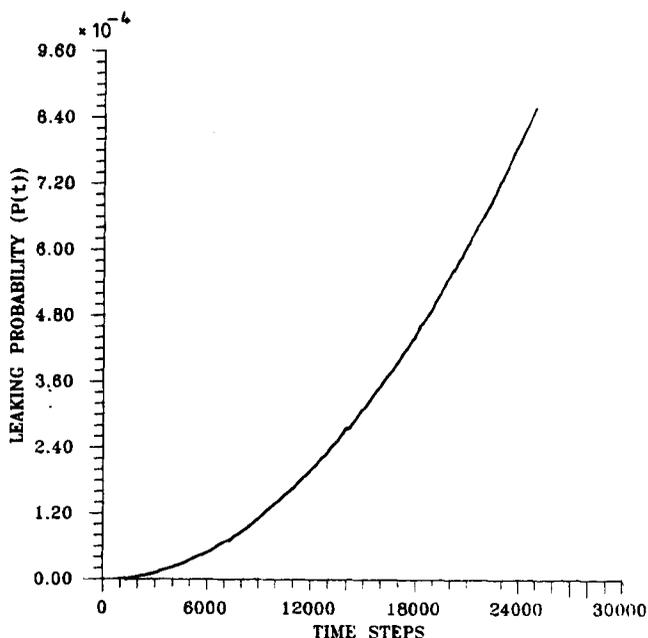where (m_1, m_2) are the left- and rightmost points on q-axis defining the left well

Figure 7. The barrier penetration probability of the H atom shown as a function of time ($\Delta t = 0.005$ fs).
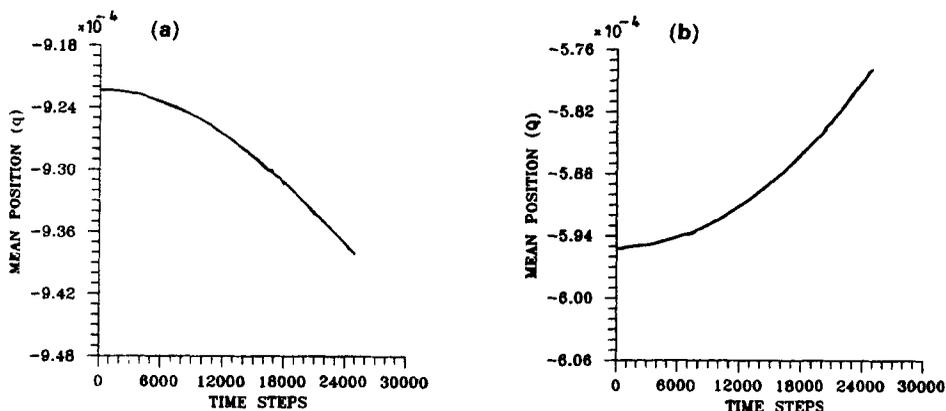

Figure 8. The mean positional coordinates of the H atom at different instants of time, (a) $\langle q(t) \rangle$, (b) $\langle Q(t) \rangle$, during the H-atom transfer in malonaldehyde (MA). Note the essentially two-dimensional nature of the tunnelling path ($\Delta t = 0.005$ fs).

perimeters while (n_1, n_2) define an identical pair on the Q axis. $dP(t)/dt$ then gives the instantaneous rate of H-atom leaking through the barrier. Thus, by fitting $P(t)$ to a form $A e^{kt}$ (figure 7) we get an estimate of the zero temperature H-atom tunnelling rate constant $(k = 6.97 \times 10^{12} s^{-1})$. From the energy splitting of the 0^+ and 0^- states, the estimated $k' \simeq \dfrac{2\Delta E}{h} = 1.5 \times 10^{10} s^{-1}$. The tunnelling rate constant (k) obtained from the dynamical method proposed by us agrees well with the available experimental and theoretical rate (Benderskii *et al* 1993; Bosch *et al* 1990). To obtain a clear idea of the nature of the path of H-atom trnsfer, we have plotted in figures 8a and b $\langle q(t) \rangle$ and $\langle Q(t) \rangle$ as functions of time. It is clear from the figures that the trajectory is two-dimensional. This feature also agrees with the result of a recent calculation by the instanton method (Benderskii *et al* 1993). Finite temperature rates can be similarly calculated by averaging k over the accessible states at the given temperature (T). However, we have restricted ourselves to the zero temperature limit in the present communication.

4. Conclusions

The TDFGH technique appears to be a quite valuable tool for studying real-time quantum dynamics in one and many dimensions. For the multidimensional cases, the Hartree type of mean-field approximation frequently works well in the TDFGH framework. But for problems where such simple product wave function is incapable of describing the state at $t = 0$, one must take linear combination of degenerate or quasi-degenerate Hartree product states and invoke a multiconfiguration time-dependent Hartree model in the FGH representation. We hope to return to this problem in a future communication.

5. Acknowledgement

References

Adhikari S and Bhattacharyya S P 1992 *Phys. Lett.* **A172** 155
Adhikari S, Dutta P and Bhattacharyya S P 1992 *Chem. Phys. Lett.* **199** 574
Adhikari S, Dutta P and Bhattacharyya S P 1993 *Chem. Phys. Lett.* (submitted)
Adhikari S, Dutta P, Sarkar P and Bhattacharyya S P 1994 *J. Phys. Chem.* (submitted)
Alimi R and Gerber R B 1990 *Phys. Rev. Lett.* **64** 1453
Balint-Kurti G G, Ward C L and Marston C C 1991 *Comput. Phys. Commun.* **67** 285
Bandrauk A D (ed.) 1988 *Atomic and molecular processes with short intense laser pulses* (New York: Plenum)
Benderskii V A, Makarov D E and Grinevich P G 1993 *Chem. Phys.* **170** 275
Bosch E, Moreno M, Lluch J M and Bertran J 1990 *J. Chem. Phys.* **93** 5685
Burnett K, Knight P L, Pivaux B R M and Reed V C 1991 *Phys. Rev. Lett.* **66** 301
Chelkowski S and Bandrauk A D 1990 *Phys. Rev.* **A41** 6480

Chelkowski S, Bandrauk A D and Corkum P B 1990 *Phys. Rev. Lett.* **65** 2335

Chu S I 1990 *Chem. Phys. Lett.* **167** 155

Coalson R D 1990 *Chem. Phys. Lett.* **165** 443

Dirac P A M 1930 *Proc. Cambridge Phil. Soc.* **26** 376

Dutta P, Adhikari S and Bhattacharyya S P 1993 *Chem. Phys. Lett.* **212** 677

Feit M D and Fleck Jr J A 1983 *J. Chem. Phys.* **78** 301

Feit M D, Fleck Jr J A and Steiger A 1982 *J. Comput. Phys.* **47** 412

Frenkel J 1934 *Wave mechanics* (Oxford: University Press)

Grochmalicki J, Lewenstein M and Pzazewski K 1991 *Phys. Rev. Lett.* **66** 1038

Kosloff R 1988 *J. Phys. Chem.* **92** 2087

Kosloff R and Tal-Ezer H 1986 *Chem. Phys. Lett.* **127** 223

Kudla Kathleen and Schatz G C 1993 *Chem. Phys.* **175** 71

Light J C, Hamilton I P and Lill J V 1985 *J. Chem. Phys.* **82** 1400

McCullough E A and Wyatt R E 1969 *J. Chem. Phys.* **51** 1253

McCullough E A and Wyatt R E 1971 *J. Chem. Phys.* **54** 3578

Makri N and Miller W H 1987 *J. Chem. Phys.* **87** 5781

Marston C C and Balint-Kurti G G 1989 *J. Chem. Phys.* **91** 3571

Messina M and Coalson R C 1990a *J. Chem. Phys.* **92** 5297

Messina M and Coalson 1990b *J. Chem. Phys.* **92** 7123

Newberger J and Noid D W 1983 *Chem. Phys. Lett.* **104** 1

Noid D M, Kosykowski M L and Marcees R A 1981 *Annu. Rev. Phys.* **32** 257

Phillips D L, Rodier J M and Mayers A B 1992 in *Time resolved vibrational spectroscopy* (ed.) H Takahashi (Berlin: Springer)

Ratner M A and Gerber R B 1986 *J. Phys. Chem.* **90** 20

Stoer J and Bulirsch R 1980 *Introduction to numerical analysis* (New York: Springer). sec. 7.2.14

Whitnell R M and Light J C 1989 *J. Chem. Phys.* **90** 1774